The important modes of subsystems: A moment-matching approach

Ben-Shan Liao[1], Zhaojun Bai[2, *, †] and Weiguo Gao[3]

[1]*Department of Mathematics, University of California, Davis, CA 95616, U.S.A.*
[2]*Department of Computer Science and Department of Mathematics, University of California, Davis, CA 95616, U.S.A.*
[3]*School of Mathematical Science, Fudan University, Shanghai 200433, People's Republic of China*

SUMMARY

Substructure coupling methods, such as the component mode synthesis (CMS) method, have been studied in structural dynamics analysis since 1960s. The modes of subsystems associated with the lowest frequencies are typically retained in these methods. In this paper, we present a coupling-matrix based mode selection scheme for the CMS method, referred to as the CMS_χ method. This new scheme is derived using a moment-matching principle defined on the interface between substructures. It is compatible to the one in recently proposed optimal modal reduction (OMR) method due to Givoli *et al*. The improvements of the CMS_χ method to the CMS and OMR methods are demonstrated by numerical examples from structural dynamics in both frequency and time domains. Copyright © 2006 John Wiley & Sons, Ltd.

1. INTRODUCTION

Substructure coupling methods as model-order reduction techniques play indispensable roles to meet the continual and compelling needs for accurately and efficiently simulating dynamical behaviour of very large structural systems. Component mode synthesis (CMS) method is one of the most popular substructure coupling methods. It employs constraint modes and fixed-interface

---

*Correspondence to: Zhaojun Bai, Department of Computer Science, University of California, Davis, CA 95616, U.S.A.
†E-mail: bai@cs.ucdavis.edu

normal modes, as presented in Hurty's method [1] and the Craig–Bampton variant of Hurty's method [2]. The CMS method explicitly exploits underlying structures of subsystems and effectively avoids the expenses of processing the entire system at once. The CMS-based model-order reduction of subsystems can be conducted in parallel, and furthermore, subsystem structure is preserved. The CMS method has its roots back to the early work of Hurty [3] in 1960. We refer to an overview paper [4] and references therein for further details. The mathematical analysis of the CMS method is in the work of Bourquin [5] and Bourquin and d'Hennezel [6, 7]. A multilevel extension, called automated multilevel substructuring (AMLS) method, is presented by Bennighof *et al.* [8–11].

Consider a lumped MIMO dynamical system of the form

$$\Sigma_N : \begin{cases} \mathbf{M}\ddot{\mathbf{x}}(t) + \mathbf{K}\mathbf{x}(t) = \mathbf{B}\mathbf{u}(t) \\ \mathbf{y}(t) \qquad\qquad = \mathbf{L}^{\mathrm{T}}\mathbf{x}(t) \end{cases} \tag{1}$$

with the initial conditions $\mathbf{x}(0) = \mathbf{x}_0$ and $\dot{\mathbf{x}}(0) = \mathbf{v}_0$. Here t is the time variable, $\mathbf{x}(t) \in \mathcal{R}^N$ is a state vector, N is the degree of freedoms, $\mathbf{u}(t) \in \mathcal{R}^p$ the input excitation force vector, and $\mathbf{y}(t) \in \mathcal{R}^m$ the output measurement vector. $\mathbf{B} \in \mathcal{R}^{N \times p}$ and $\mathbf{L} \in \mathcal{R}^{N \times m}$ are input and output distribution arrays, respectively. $\mathbf{M}$ and $\mathbf{K}$ are mass and stiffness matrices. Assume that $\mathbf{M}$ is symmetric semidefinite and $\mathbf{K}$ is symmetric positive definite. Furthermore, the state vector $\mathbf{x}(t)$ and the system matrices $\mathbf{M}$ and $\mathbf{K}$ are composed of subsystem structures, namely, they are partitioned into three blocks, representing subsystems I, II and their interface

$$\mathbf{x}(t) = \begin{bmatrix} \mathbf{x}_1(t) \\ \mathbf{x}_2(t) \\ \mathbf{x}_3(t) \end{bmatrix}, \quad \mathbf{M} = \begin{bmatrix} \mathbf{M}_{11} & & \mathbf{M}_{13} \\ & \mathbf{M}_{22} & \mathbf{M}_{23} \\ \mathbf{M}_{13}^{\mathrm{T}} & \mathbf{M}_{23}^{\mathrm{T}} & \mathbf{M}_{33} \end{bmatrix}, \quad \mathbf{K} = \begin{bmatrix} \mathbf{K}_{11} & & \mathbf{K}_{13} \\ & \mathbf{K}_{22} & \mathbf{K}_{23} \\ \mathbf{K}_{13}^{\mathrm{T}} & \mathbf{K}_{23}^{\mathrm{T}} & \mathbf{K}_{33} \end{bmatrix} \tag{2}$$

The degrees of freedom of subsystems I, II and the interface are denoted by N_1, N_2 and N_3, respectively. Thus, the degree of freedoms of the entire system Σ_N is $N = N_1 + N_2 + N_3$. The input–output behaviour of Σ_N in frequency domain is characterized by the m-by-p transfer matrix [12]

$$\mathbf{H}(\omega) = \mathbf{L}^{\mathrm{T}}(-\omega^2\mathbf{M} + \mathbf{K})^{-1}\mathbf{B}$$

where ω is referred to as the frequency.

A substructure coupling method first computes a few selected (eigen)modes of the subsystems, and then derives a system Σ_n of the same form but a (much) smaller dimension of the state vector $\mathbf{z}(t)$ by a projection (see Section 2 for detail)

$$\Sigma_n : \begin{cases} \mathbf{M}_n\ddot{\mathbf{z}}(t) + \mathbf{K}_n\mathbf{z}(t) = \mathbf{B}_n\mathbf{u}(t) \\ \mathbf{y}_n(t) \qquad\qquad = \mathbf{L}_n^{\mathrm{T}}\mathbf{z}(t) \end{cases} \tag{3}$$

where the degree of freedoms of the new state vector $\mathbf{z}(t)$ is $n = n_1 + n_2 + N_3$ with $n_1 \leqslant N_1$ and $n_2 \leqslant N_2$. We assume that the degree of freedoms of the interface is unchanged. The reduced system matrices $\mathbf{M}_n$ and $\mathbf{K}_n$ preserve the block structures of the original system matrices $\mathbf{M}$ and $\mathbf{K}$, i.e.

$$\mathbf{M}_n = \begin{bmatrix} \mathbf{M}_{11}^{(n)} & & \mathbf{M}_{13}^{(n)} \\ & \mathbf{M}_{22}^{(n)} & \mathbf{M}_{23}^{(n)} \\ (\mathbf{M}_{13}^{(n)})^{\mathrm{T}} & (\mathbf{M}_{23}^{(n)})^{\mathrm{T}} & \widehat{\mathbf{M}}_{33} \end{bmatrix} \quad \text{and} \quad \mathbf{K}_n = \begin{bmatrix} \mathbf{K}_{11}^{(n)} & & \mathbf{K}_{13}^{(n)} \\ & \mathbf{K}_{22}^{(n)} & \mathbf{K}_{23}^{(n)} \\ (\mathbf{K}_{13}^{(n)})^{\mathrm{T}} & (\mathbf{K}_{23}^{(n)})^{\mathrm{T}} & \widehat{\mathbf{K}}_{33} \end{bmatrix} \tag{4}$$

Correspondingly, the input–output behaviour of the reduced system Σ_n in frequency domain is characterized by the m-by-p transfer function

$$\mathbf{H}_n(\omega) = \mathbf{L}_n^{\mathrm{T}}(-\omega^2 \mathbf{M}_n + \mathbf{K}_n)^{-1}\mathbf{B}_n$$

It is necessary that the input–output behaviour of the reduced system Σ_n is an acceptable approximation of the original system Σ_N.

The quality of such a substructure coupling method essentially relies on the modes of subsystems selected to retain. A standard mode selection practice is to retain the modes associated with a few lowest frequencies. However, this mode selection does not necessarily produce an optimal reduced system Σ_n. Let us use the following simple example to illustrate this. Let the system Σ_N be given by

$$\mathbf{M} = \begin{bmatrix} 1 & & & 0.7 \\ & 1 & & 10^{-3} \\ & & 1 & 0.3 \\ 0.7 & 10^{-3} & 0.3 & 1 \end{bmatrix}, \quad \mathbf{K} = \begin{bmatrix} 0.9 & & & \\ & 1 & & \\ & & 2 & \\ & & & 1 \end{bmatrix}, \quad \mathbf{B} = \begin{bmatrix} 1 \\ 0 \\ 0 \\ 0 \end{bmatrix}, \quad \mathbf{L} = \begin{bmatrix} 1 \\ 0 \\ 0 \\ 0 \end{bmatrix} \quad (5)$$

Suppose the subsystem II is reduced. Then by the lowest frequency mode selection criterion, the reduced system Σ_n is given by

$$\mathbf{M}_n = \begin{bmatrix} 1 & & 0.7 \\ & 1 & 10^{-3} \\ 0.7 & 10^{-3} & 1 \end{bmatrix}, \quad \mathbf{K}_n = \begin{bmatrix} 0.9 & & \\ & 1 & \\ & & 1 \end{bmatrix}, \quad \mathbf{B}_n = \begin{bmatrix} 1 \\ 0 \\ 0 \end{bmatrix}, \quad \mathbf{L}_n = \begin{bmatrix} 1 \\ 0 \\ 0 \end{bmatrix} \quad (6)$$

Alternatively, if we retain the other mode in the subsystem II, then the reduced system Σ_n^{χ} is given by

$$\mathbf{M}_n^{\chi} = \begin{bmatrix} 1 & & 0.7 \\ & 1 & 0.3 \\ 0.7 & 0.3 & 1 \end{bmatrix}, \quad \mathbf{K}_n^{\chi} = \begin{bmatrix} 0.9 & & \\ & 2 & \\ & & 1 \end{bmatrix}, \quad \mathbf{B}_n^{\chi} = \begin{bmatrix} 1 \\ 0 \\ 0 \end{bmatrix}, \quad \mathbf{L}_n^{\chi} = \begin{bmatrix} 1 \\ 0 \\ 0 \end{bmatrix} \quad (7)$$

The left of Figure 1 shows the magnitudes (in log of base 10) of the transfer functions $\mathbf{H}(\omega)$, $\mathbf{H}_n(\omega)$ and $\mathbf{H}_n^{\chi}(\omega)$ of the original system Σ_N, and the reduced systems Σ_n and Σ_n^{χ}. The right of Figure 1 shows the output $y(t)$ of Σ_N and the reduced ones $y_n(t)$ of Σ_n and $y_n^{\chi}(t)$ of Σ_n^{χ} with the input function $\mathbf{u}(t) = \cos(t)$. It is clear that the low-frequency dominant mode selection practice is not optimal.

A question that arises naturally is '*which are the important modes of subsystems*?' In the recent work of Barbone and Givoli [13] and Givoli *et al.* [14], an optimal modal reduction (OMR) algorithm is proposed. In contrast to the low-frequency dominant mode selection rule, a *coupling matrix*-based mode selection criterion is introduced. It is derived *via* the DtN map [15], originally developed for solving partial differential equations with non-reflecting boundary conditions [16].

In this paper, inspired by the OMR method, we present an alternative mode selection criterion for the CMS method. The resulting method is called CMS$_{\chi}$, where χ stands for variation. Instead of using the DtN map [15], we derive the CMS$_{\chi}$-mode selection criterion in an algebraic setting and use the moment-matching principle in frequency domain. The improvements of the CMS$_{\chi}$ method to the CMS and OMR methods will be demonstrated by numerical examples from structural dynamics in both frequency and time domains.
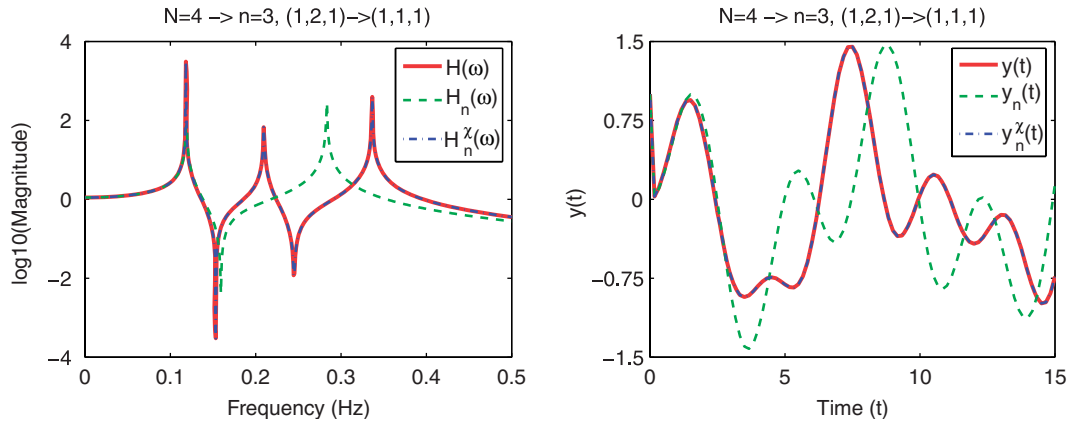
Figure 1. Left: transfer functions of systems Σ_N, Σ_n and Σ_n^χ in frequency domain. Right: outputs of systems Σ_N, Σ_n and Σ_n^χ in time domain.

The rest of the paper is organized as follows. Section 2 reviews the CMS method and presents a new variation of CMS method, called CMS$_\chi$. The derivation and justification of the CMS$_\chi$ method are in Section 3. Section 4 applies CMS$_\chi$ to the case of only one subsystem reduction and compares with the OMR method. Numerical examples are presented in Section 5. Concluding remarks are in Section 6.

2. SUBSTRUCTURING METHODS

In this section, we first review the CMS method in an algebraic setting. Then we present a variation of the CMS method, referred to as the CMS$_\chi$ method. The derivation and justification of the CMS$_\chi$ method are presented in the next section.

The CMS method consists of two key steps: (a) applying a congruence transformation to transform the matrix pair $(\mathbf{M}, \mathbf{K})$ to the so-called Craig–Bampton form with the matrix

$$
\mathbf{U} = \begin{array}{c} N_1 \\ N_2 \\ N_3 \end{array} \overset{\begin{array}{ccc} N_1 & N_2 & N_3 \end{array}}{\left(\begin{array}{ccc} \mathbf{I} & & \mathbf{\Psi}_{13} \\ & \mathbf{I} & \mathbf{\Psi}_{23} \\ & & \mathbf{I} \end{array} \right)} \tag{8}
$$

where $\mathbf{\Psi}_{13} = -\mathbf{K}_{11}^{-1}\mathbf{K}_{13}$ and $\mathbf{\Psi}_{23} = -\mathbf{K}_{22}^{-1}\mathbf{K}_{23}$, and (b) projecting the Craig–Bampton form onto the subspace spanned by the matrix $\mathbf{V}_n$

$$
\mathbf{V}_n = \begin{array}{c} N_1 \\ N_2 \\ N_3 \end{array} \overset{\begin{array}{ccc} n_1 & n_2 & N_3 \end{array}}{\left(\begin{array}{ccc} \mathbf{\Phi}_1 & & \\ & \mathbf{\Phi}_2 & \\ & & \mathbf{I} \end{array} \right)} \tag{9}
$$

where for $i = 1, 2$, $\mathbf{\Phi}_i$ is an $N_i \times n_i$ matrix whose columns are the selected n_i eigenvectors $\mathbf{\phi}_j^{(i)}$ of the submatrix pairs $(\mathbf{M}_{ii}, \mathbf{K}_{ii})$

$$\mathbf{K}_{ii} \mathbf{\phi}_j^{(i)} = \lambda_j^{(i)} \mathbf{M}_{ii} \mathbf{\phi}_j^{(i)} \tag{10}$$

with

$$(\mathbf{\phi}_j^{(i)})^{\mathrm{T}} \mathbf{M}_{ii} \mathbf{\phi}_k^{(i)} = \delta_{jk} = \begin{cases} 1 & \text{if } j = k \\ 0 & \text{otherwise} \end{cases} \tag{11}$$

In structural dynamics, $\mathbf{\Psi}_{i3}$ are referred to as interior partition of the constraint-mode matrices and $\mathbf{\Phi}_i$ are called the interior partition of the fixed-interface modal matrices.

Specifically, by performing a congruence transformation on Σ_N with the matrix $\mathbf{U}$, it yields an equivalent system

$$\widehat{\Sigma}_N : \begin{cases} \widehat{\mathbf{M}} \ddot{\widehat{\mathbf{x}}}(t) + \widehat{\mathbf{K}} \widehat{\mathbf{x}}(t) = \widehat{\mathbf{B}} u(t) \\ \mathbf{y}(t) \qquad\qquad = \widehat{\mathbf{L}}^{\mathrm{T}} \widehat{\mathbf{x}}(t) \end{cases} \tag{12}$$

where $\widehat{\mathbf{x}}(t) = \mathbf{U}^{-1} \mathbf{x}(t)$. System matrices $\widehat{\mathbf{M}} = \mathbf{U}^{\mathrm{T}} \mathbf{M} \mathbf{U}$ and $\widehat{\mathbf{K}} = \mathbf{U}^{\mathrm{T}} \mathbf{K} \mathbf{U}$, and the input–output influence arrays $\widehat{\mathbf{B}} = \mathbf{U}^{\mathrm{T}} \mathbf{B}$ and $\widehat{\mathbf{L}} = \mathbf{U}^{\mathrm{T}} \mathbf{L}$ have the following structures:

$$\widehat{\mathbf{M}} = \begin{bmatrix} \mathbf{M}_{11} & & \widehat{\mathbf{M}}_{13} \\ & \mathbf{M}_{22} & \widehat{\mathbf{M}}_{23} \\ \widehat{\mathbf{M}}_{13}^{\mathrm{T}} & \widehat{\mathbf{M}}_{23}^{\mathrm{T}} & \widehat{\mathbf{M}}_{33} \end{bmatrix}, \quad \widehat{\mathbf{K}} = \begin{bmatrix} \mathbf{K}_{11} & & \\ & \mathbf{K}_{22} & \\ & & \widehat{\mathbf{K}}_{33} \end{bmatrix}, \quad \widehat{\mathbf{B}} = \begin{bmatrix} \mathbf{B}_1 \\ \mathbf{B}_2 \\ \widehat{\mathbf{B}}_3 \end{bmatrix}, \quad \widehat{\mathbf{L}} = \begin{bmatrix} \mathbf{L}_1 \\ \mathbf{L}_2 \\ \widehat{\mathbf{L}}_3 \end{bmatrix} \tag{13}$$

where

$$\widehat{\mathbf{M}}_{i3} = \mathbf{M}_{i3} - \mathbf{M}_{ii} \mathbf{K}_{ii}^{-1} \mathbf{K}_{i3} \quad \text{for } i = 1, 2$$

$$\widehat{\mathbf{M}}_{33} = \mathbf{M}_{33} - \sum_{i=1}^{2} (\mathbf{K}_{i3}^{\mathrm{T}} \mathbf{K}_{ii}^{-1} \mathbf{M}_{i3} + \mathbf{M}_{i3}^{\mathrm{T}} \mathbf{K}_{ii}^{-1} \mathbf{K}_{i3} - \mathbf{K}_{i3}^{\mathrm{T}} \mathbf{K}_{ii}^{-1} \mathbf{M}_{ii} \mathbf{K}_{ii}^{-1} \mathbf{K}_{i3})$$

$$\widehat{\mathbf{K}}_{33} = \mathbf{K}_{33} - \mathbf{K}_{13}^{\mathrm{T}} \mathbf{K}_{11}^{-1} \mathbf{K}_{13} - \mathbf{K}_{23}^{\mathrm{T}} \mathbf{K}_{22}^{-1} \mathbf{K}_{23}$$

$$\widehat{\mathbf{B}}_3 = \mathbf{B}_3 - \mathbf{K}_{13}^{\mathrm{T}} \mathbf{K}_{11}^{-1} \mathbf{B}_1 - \mathbf{K}_{23}^{\mathrm{T}} \mathbf{K}_{22}^{-1} \mathbf{B}_2$$

$$\widehat{\mathbf{L}}_3 = \mathbf{L}_3 - \mathbf{K}_{13}^{\mathrm{T}} \mathbf{K}_{11}^{-1} \mathbf{L}_1 - \mathbf{K}_{23}^{\mathrm{T}} \mathbf{K}_{22}^{-1} \mathbf{L}_2$$

The matrix pair $(\widehat{\mathbf{M}}, \widehat{\mathbf{K}})$ is called the Craig–Bampton form [2]. In the continuous variational setting, $\widehat{\mathbf{M}}_{33}$ is a discrete version of the mass complement operator [10] and $\widehat{\mathbf{K}}_{33}$ is the discrete version of the Steklov–Poincaré operator [17].

An orthogonal projection technique for dimension reduction seeks an approximation of $\widehat{\mathbf{x}}(t)$ constrained to stay in the subspace spanned by the columns of $\mathbf{V}_n$, namely

$$\widehat{\mathbf{x}}(t) \approx \mathbf{V}_n \mathbf{z}(t)$$

Then by imposing the Galerkin orthogonal condition

$$\widehat{\mathbf{M}} \mathbf{V}_n \ddot{\mathbf{z}}(t) + \widehat{\mathbf{K}} \mathbf{V}_n \mathbf{z}(t) - \widehat{\mathbf{B}} u(t) \perp \text{span}\{\mathbf{V}_n\}$$

it yields a reduced-order system of the form

$$\Sigma_n : \begin{cases} \mathbf{M}_n\ddot{\mathbf{z}}(t) + \mathbf{K}_n\mathbf{z}(t) = \mathbf{B}_n\mathbf{u}(t) \\ \hat{\mathbf{y}}(t) \qquad\qquad\;\; = \mathbf{L}_n^{\mathrm{T}}\mathbf{z}(t) \end{cases} \tag{14}$$

where $\mathbf{M}_n = \mathbf{V}_n^{\mathrm{T}}\widehat{\mathbf{M}}\mathbf{V}_n$, $\mathbf{K}_n = \mathbf{V}_n^{\mathrm{T}}\widehat{\mathbf{K}}\mathbf{V}_n$, $\mathbf{B}_n = \mathbf{V}_n^{\mathrm{T}}\widehat{\mathbf{B}}$ and $\mathbf{L}_n = \mathbf{V}_n^{\mathrm{T}}\widehat{\mathbf{L}}$. By the definition of $\mathbf{V}_n$, the matrices $\mathbf{M}_n$ and $\mathbf{K}_n$ are of the forms

$$\mathbf{M}_n = \begin{bmatrix} \mathbf{I} & & \mathbf{M}_{13}^{(n)} \\ & \mathbf{I} & \mathbf{M}_{23}^{(n)} \\ (\mathbf{M}_{13}^{(n)})^{\mathrm{T}} & (\mathbf{M}_{23}^{(n)})^{\mathrm{T}} & \widehat{\mathbf{M}}_{33} \end{bmatrix}, \quad \mathbf{K}_n = \begin{bmatrix} \mathbf{\Lambda}_1^{(n)} & & \\ & \mathbf{\Lambda}_2^{(n)} & \\ & & \widehat{\mathbf{K}}_{33} \end{bmatrix} \tag{15}$$

with $\mathbf{M}_{13}^{(n)} = \mathbf{\Phi}_1^{\mathrm{T}}\widehat{\mathbf{M}}_{13}$ and $\mathbf{M}_{23}^{(n)} = \mathbf{\Phi}_2^{\mathrm{T}}\widehat{\mathbf{M}}_{23}$.

A high-level description of the CMS method is as follows:

Algorithm 1: CMS method

1. Transform $(\mathbf{M}, \mathbf{K})$ to Craig–Bampton form $(\widehat{\mathbf{M}}, \widehat{\mathbf{K}})$ as in (13).
2. For $i = 1, 2$, compute the n_i lowest eigenpairs $(\lambda_j^{(i)}, \boldsymbol{\phi}_j^{(i)})$ of i-th subsystem $(\mathbf{K}_{ii}, \mathbf{M}_{ii})$, and define the matrix $\mathbf{\Phi}_i$ as in (9), where the eigenvalues $\lambda_j^{(i)}$ are ordered in increasing order $\lambda_1^{(i)} \leqslant \lambda_2^{(i)} \leqslant \cdots \leqslant \lambda_{N_i}^{(i)}$.
3. Form $\mathbf{M}_n, \mathbf{K}_n, \mathbf{B}_n, \mathbf{L}_n$ to define the reduced system Σ_n as in (14).

A question that arises naturally is whether the CMS strategy of the mode selection of subsystems is optimal, or '*which are the important modes of subsystems*?' We will show in the next section that a better mode selection strategy is to introduce a *coupling matrix* $\mathbf{S}_j^{(i)}$ associated with the jth mode of the subsystem i

$$\mathbf{S}_j^{(i)} = \frac{1}{\lambda_j^{(i)}} \widehat{\mathbf{M}}_{i3}^{\mathrm{T}} \boldsymbol{\phi}_j^{(i)} (\boldsymbol{\phi}_j^{(i)})^{\mathrm{T}} \widehat{\mathbf{M}}_{i3} \tag{16}$$

The n_i modes $\boldsymbol{\phi}_j^{(i)}$ of subsystem i are then selected according to the largest norms of their corresponding *coupling matrices* $\mathbf{S}_j^{(i)}$. Let us refer to this variation of the CMS method as the CMS_χ method. The following is a high-level description of the CMS_χ method.

Algorithm 2: CMS_χ *method*

1. Transform $(\mathbf{M}, \mathbf{K})$ to Craig–Bampton form $(\widehat{\mathbf{M}}, \widehat{\mathbf{K}})$ (13).
2. For $i = 1, 2$, compute the eigenpairs $(\lambda_j^{(i)}, \boldsymbol{\phi}_j^{(i)})$ of i-th subsystem $(\mathbf{K}_{ii}, \mathbf{M}_{ii})$.
3. Sort the eigenpairs $(\lambda_j^{(i)}, \boldsymbol{\phi}_j^{(i)})$ according to the norms of the *coupling matrices* $\mathbf{S}_j^{(i)}$ in descending order, i.e.

$$\|\mathbf{S}_1^{(i)}\| \geqslant \|\mathbf{S}_2^{(i)}\| \geqslant \cdots \geqslant \|\mathbf{S}_{N_i}^{(i)}\|$$

4. Retain first n_i eigenpairs $(\lambda_j^{(i)}, \boldsymbol{\phi}_j^{(i)})$ to define the matrix $\boldsymbol{\Phi}_i$ (9).
5. Form $\mathbf{M}_n, \mathbf{K}_n, \mathbf{B}_n, \mathbf{L}_n$ to define the reduced system Σ_n (14).

We note that the matrix 2-norm is used at step 3 of the CMS_χ method, the 2-norm of the coupling matrix $\mathbf{S}_j^{(i)}$ is simply given by

$$\|\mathbf{S}_j^{(i)}\| = \frac{1}{\lambda_j^{(i)}} \|\widehat{\mathbf{M}}_{i3}^{\mathrm{T}} \boldsymbol{\phi}_j^{(i)}\|^2$$

due to the fact that the coupling matrix $\mathbf{S}_j^{(i)}$ is symmetric and of rank-one.

Note that the difference between the CMS and CMS_χ methods is only in the mode selection of subsystems. The selected modes $\boldsymbol{\phi}_j^{(i)}$ in CMS_χ are not in the natural order as in CMS. As a result, to find such n_i modes, we may have to find more than n_i smallest eigenpairs of the matrix pairs $(\mathbf{M}_{ii}, \mathbf{K}_{ii})$. This will be shown by numerical examples in Section 5.

3. DERIVATION OF CMS_χ

Let $\boldsymbol{\Phi}_i$ contain all N_i modes of the submatrix pairs $(\mathbf{M}_{ii}, \mathbf{K}_{ii})$ for $i = 1, 2$. Then in frequency domain, the system Σ_N with the impulse input function in its modal co-ordinate is of the form

$$\left(-\omega^2 \begin{bmatrix} \mathbf{I} & & \mathbf{M}_{13}^{(N)} \\ & \mathbf{I} & \mathbf{M}_{23}^{(N)} \\ (\mathbf{M}_{13}^{(N)})^{\mathrm{T}} & (\mathbf{M}_{23}^{(N)})^{\mathrm{T}} & \widehat{\mathbf{M}}_{33} \end{bmatrix} + \begin{bmatrix} \boldsymbol{\Lambda}_1^{(N)} & & \\ & \boldsymbol{\Lambda}_2^{(N)} & \\ & & \widehat{\mathbf{K}}_{33} \end{bmatrix}\right) \begin{bmatrix} \mathbf{X}_1(\omega) \\ \mathbf{X}_2(\omega) \\ \mathbf{X}_3(\omega) \end{bmatrix} = \begin{bmatrix} \mathbf{B}_1^{(N)} \\ \mathbf{B}_2^{(N)} \\ \widehat{\mathbf{B}}_3 \end{bmatrix} \quad (17)$$

For the sake of notation, we will drop the superscript (N) in the rest of section. By solving $\mathbf{X}_1(\omega)$ and $\mathbf{X}_2(\omega)$ from the first and second equations of (17) and then substituting into the third interface equation of (17), it yields

$$\left(-\omega^4 \sum_{i=1}^{2} [\mathbf{M}_{i3}^{\mathrm{T}}(-\omega^2\mathbf{I} + \boldsymbol{\Lambda}_i)^{-1}\mathbf{M}_{i3}] - \omega^2\widehat{\mathbf{M}}_{33} + \widehat{\mathbf{K}}_{33}\right) \mathbf{X}_3(\omega)$$

$$= \left(\omega^2 \sum_{i=1}^{2} [\mathbf{M}_{i3}^{\mathrm{T}}(-\omega^2\mathbf{I} + \boldsymbol{\Lambda}_i)^{-1}\mathbf{B}_i] + \widehat{\mathbf{B}}_3\right) \quad (18)$$

In the context of structural dynamics, Equation (18) represents the accumulation of the forces applied to the interface.

Instead of solving Equation (18) for $\mathbf{X}_3(\omega)$ directly, we first simplify the equation to look for a few 'important' modes. An approximation of (18) can be obtained by keeping the first three terms of the power expansion in ω^2 of the coefficient matrix on the left hand side and the constant term on the right hand side. This yields an approximate equation of (18)

$$[-\omega^4(\mathbf{M}_{13}^{\mathrm{T}}\boldsymbol{\Lambda}_1^{-1}\mathbf{M}_{13} + \mathbf{M}_{23}^{\mathrm{T}}\boldsymbol{\Lambda}_2^{-1}\mathbf{M}_{23}) - \omega^2\widehat{\mathbf{M}}_{33} + \widehat{\mathbf{K}}_{33}]\widetilde{\mathbf{X}}_3(\omega) = \widehat{\mathbf{B}}_3 \quad (19)$$

Let the power series expansion of $\widetilde{\mathbf{X}}_3(\omega)$ be formally denoted by

$$\widetilde{\mathbf{X}}_3(\omega) = \sum_{\ell=0}^{\infty} \mathbf{r}_\ell \omega^{2\ell}$$

where $\mathbf{r}_\ell$ are called the ℓth moment vector of $\widetilde{\mathbf{X}}_3(\omega)$. Then by comparing the two sides of Equation (19) in the power of ω^2, we observe that the moment vectors $\mathbf{r}_\ell$ are given by the second-order recurrence

$$\mathbf{r}_\ell = [\widehat{\mathbf{K}}_{33}^{-1}\widehat{\mathbf{M}}_{33}]\,\mathbf{r}_{\ell-1} + \left[\widehat{\mathbf{K}}_{33}^{-1}\left(\sum_{i=1}^{2}\mathbf{M}_{i3}^{\mathrm{T}}\Lambda_i^{-1}\mathbf{M}_{i3}\right)\right]\mathbf{r}_{\ell-2}\quad\text{for }\ell\geqslant 2$$

with initial moment vectors $\mathbf{r}_0 = \widehat{\mathbf{K}}_{33}^{-1}\widehat{\mathbf{B}}_3$ and $\mathbf{r}_1 = \widehat{\mathbf{K}}_{33}^{-1}\widehat{\mathbf{M}}_{33}\mathbf{r}_0$.

By an analogous calculation, for the reduced-order system Σ_n in its modal co-ordinate form

$$\left(-\omega^2\begin{bmatrix}\mathbf{I} & & \mathbf{M}_{13}^{(n)}\\ & \mathbf{I} & \mathbf{M}_{23}^{(n)}\\ (\mathbf{M}_{13}^{(n)})^{\mathrm{T}} & (\mathbf{M}_{23}^{(n)})^{\mathrm{T}} & \mathbf{M}_{33}^{(n)}\end{bmatrix} + \begin{bmatrix}\Lambda_1^{(n)} & & \\ & \Lambda_2^{(n)} & \\ & & \mathbf{K}_{33}^{(n)}\end{bmatrix}\right)\begin{bmatrix}\mathbf{X}_1^{(n)}(\omega)\\ \mathbf{X}_2^{(n)}(\omega)\\ \mathbf{X}_3^{(n)}(\omega)\end{bmatrix} = \begin{bmatrix}\mathbf{B}_1^{(n)}\\ \mathbf{B}_2^{(n)}\\ \widehat{\mathbf{B}}_3^{(n)}\end{bmatrix}\quad(20)$$

the moment vectors $\mathbf{r}_\ell^{(n)}$ of the solution $\widetilde{\mathbf{X}}_3^{(n)}(\omega)$ of the approximate interface equation are given by the second-order recurrence

$$\mathbf{r}_\ell^{(n)} = [(\mathbf{K}_{33}^{(n)})^{-1}\mathbf{M}_{33}^{(n)}]\,\mathbf{r}_{\ell-1}^{(n)} + \left[(\mathbf{K}_{33}^{(n)})^{-1}\left(\sum_{i=1}^{2}(\mathbf{M}_{i3}^{(n)})^{\mathrm{T}}(\Lambda_i^{(n)})^{-1}\mathbf{M}_{i3}^{(n)}\right)\right]\mathbf{r}_{\ell-2}^{(n)}\quad\text{for }\ell\geqslant 2$$

with initial moment vectors $\mathbf{r}_0^{(n)} = (\mathbf{K}_{33}^{(n)})^{-1}\mathbf{B}_3^{(n)}$ and $\mathbf{r}_1^{(n)} = (\mathbf{K}_{33}^{(n)})^{-1}\mathbf{M}_{33}^{(n)}\mathbf{r}_0^{(n)}$.

Note that the dimensions of the moment vectors $\{\mathbf{r}_\ell\}$ of the original system Σ_N and the moment vectors $\{\mathbf{r}_\ell^{(n)}\}$ of the reduced-order system Σ_n are the same since it is assumed that the degree of freedoms of the interface block is unchanged. A natural optimal strategy is to match as many moment vectors $\{\mathbf{r}_\ell\}$ and $\{\mathbf{r}_\ell^{(n)}\}$ as possible. To match the first moment vector $\mathbf{r}_0 = \mathbf{r}_0^{(n)}$, we simply let

$$\mathbf{K}_{33}^{(n)} = \widehat{\mathbf{K}}_{33}\quad\text{and}\quad\mathbf{B}_3^{(n)} = \widehat{\mathbf{B}}_3$$

To match the second moment vector $\mathbf{r}_1 = \mathbf{r}_1^{(n)}$, we let

$$\mathbf{M}_{33}^{(n)} = \widehat{\mathbf{M}}_{33}$$

Unfortunately, it appears that there is no easy way to match the third moment vector $\mathbf{r}_2$ exactly. Instead, we try to minimize the difference between $\mathbf{r}_2$ and $\mathbf{r}_2^{(n)}$. By an algebraic manipulation,

it can be shown that

$$\|\mathbf{r}_2 - \mathbf{r}_2^{(n)}\| = \left\| \widehat{\mathbf{K}}_{33}^{-1} \left(\sum_{i=1}^{2} \mathbf{M}_{i3}^{\mathrm{T}} \Lambda_i^{-1} \mathbf{M}_{i3} - (\mathbf{M}_{i3}^{(n)})^{\mathrm{T}} (\Lambda_i^{(n)})^{-1} \mathbf{M}_{i3}^{(n)} \right) \widehat{\mathbf{K}}_{33}^{-1} \widehat{\mathbf{B}}_3 \right\|$$

$$\leqslant c \left\| \sum_{i=1}^{2} \widehat{\mathbf{M}}_{i3}^{\mathrm{T}} \Phi_i \Lambda_i^{-1} \Phi_i^{\mathrm{T}} \widehat{\mathbf{M}}_{i3} - \widehat{\mathbf{M}}_{i3}^{\mathrm{T}} \Phi_i^{(n)} (\Lambda_i^{(n)})^{-1} (\Phi_i^{(n)})^{\mathrm{T}} \widehat{\mathbf{M}}_{i3} \right\|$$

$$= c \left\| \underbrace{\sum_{j=1}^{N_1} \mathbf{S}_j^{(1)} - \sum_{j=1}^{n_1} (\mathbf{S}_j^{(1)})^{(n)}}_{1} + \underbrace{\sum_{j=1}^{N_2} \mathbf{S}_j^{(2)} - \sum_{j=1}^{n_2} (\mathbf{S}_j^{(2)})^{(n)}}_{2} \right\| \tag{21}$$

where $c = \|\widehat{\mathbf{K}}_{33}^{-1}\| \, \|\widehat{\mathbf{K}}_{33}^{-1}\widehat{\mathbf{B}}_3\|$, a constant independent of the modes $\phi_j^{(i)}$. $\mathbf{S}_j^{(i)}$ and $(\mathbf{S}_j^{(i)})^{(n)}$ are the coupling matrices for the jth mode of the subsystem i as defined in (16). Assume that the norms of the coupling matrices $\mathbf{S}_j^{(i)}$ and $(\mathbf{S}_j^{(i)})^{(n)}$ are in descending order, respectively

$$\|\mathbf{S}_1^{(i)}\| \geqslant \|\mathbf{S}_2^{(i)}\| \geqslant \cdots \geqslant \|\mathbf{S}_{N_i}^{(i)}\|, \quad \|(\mathbf{S}_1^{(i)})^{(n)}\| \geqslant \|(\mathbf{S}_2^{(i)})^{(n)}\| \geqslant \cdots \geqslant \|(\mathbf{S}_{n_i}^{(i)})^{(n)}\|$$

The best we can do is to set

$$(\mathbf{S}_j^{(i)})^{(n)} = \mathbf{S}_j^{(i)} \quad \text{for } j = 1, 2, \ldots, n_i$$

This cancels out the first n_i terms of the differences labelled as 1 and 2 of the upper bound in (21), and leaves the sums of the remaining terms as small as possible. By this observation, we derive the CMS$_\chi$-mode selection rule as we described in Section 2: *retain the first n_i modes of the subsystem i according to the largest norms of the coupling matrices $\mathbf{S}_j^{(i)}$*.

Note that the matrices $\widehat{\mathbf{M}}_{i3}$ which couple subsystems and the interface are included in the coupling matrices $\mathbf{S}_j^{(i)}$. They are reflected for the retention of modes of importance. These coupling effects are essentially ignored by the CMS mode selection. To this end, we also note that CMS$_\chi$-mode selection criterion is analogous to the one in the OMR method derived by the DtN map [13, 14]. The derivation presented in this section is conduced in the frequency domain. In the next section, we will show the connection between the two methods in detail. This moment-matching based mode selection derivation is simple yet powerful. Comparing to the derivation as presented in [13, 14], CMS$_\chi$-mode selection is derived without the assumption of the special form of the external force term $\mathbf{B}u(t)$ in the original system Σ_N (1). Furthermore, CMS$_\chi$-mode selection criterion is derived without the assumption of only one subsystem reduction at a time. On the other hand, the OMR mode selection is shown to be optimal in a certain sense [13], which we cannot claim for the CMS$_\chi$-mode selection.

4. ONE SUBSYSTEM REDUCTION WITHOUT MODIFYING OTHERS

In this section, we consider the setting where the OMR method [13, 14] is derived. Let subsystem I be a main system and subsystem II be a subsystem. The OMR method is developed to reduce the computational effort associated with the dynamic analysis of a linear subsystem 'attached'

to a main system. Only the dynamic behaviour of the main system is of great interest when a reduction is performed on the subsystem alone without modifying the main system. It is assumed that all the external loading is applied to the main system and thus the subsystem and the interface are unloaded externally. To accurately represent the effect on the dynamic behaviour of the main system by subsystems, it is further assumed that all non-zero initial conditions apply to the main system.

In order to preserve the structure of the original system without modifying main system, the reduction of the matrices $\mathbf{M}$ and $\mathbf{K}$ of the original system Σ_N are replaced by the smaller matrices $\mathbf{M}_n$ and $\mathbf{K}_n$ of the following forms:

$$\mathbf{M}_n = \begin{bmatrix} \mathbf{M}_{11} & & \mathbf{M}_{13} \\ & \mathbf{M}_{22}^{(n)} & \mathbf{M}_{23}^{(n)} \\ \mathbf{M}_{13}^{\mathrm{T}} & (\mathbf{M}_{23}^{(n)})^{\mathrm{T}} & \widehat{\mathbf{M}}_{33} \end{bmatrix} \quad \text{and} \quad \mathbf{K}_n = \begin{bmatrix} \mathbf{K}_{11} & & \mathbf{K}_{13} \\ & \mathbf{K}_{22}^{(n)} & \mathbf{K}_{23}^{(n)} \\ \mathbf{K}_{13}^{\mathrm{T}} & (\mathbf{K}_{23}^{(n)})^{\mathrm{T}} & \widehat{\mathbf{K}}_{33} \end{bmatrix} \tag{22}$$

where the block matrices $\mathbf{M}_{22}, \mathbf{M}_{23}, \mathbf{M}_{33}, \mathbf{K}_{22}, \mathbf{K}_{23}$ and $\mathbf{K}_{33}$ of Σ_N are replaced by $\mathbf{M}_{22}^{(n)}, \mathbf{M}_{23}^{(n)}$, $\widehat{\mathbf{M}}_{33}, \mathbf{K}_{22}^{(n)}, \mathbf{K}_{23}^{(n)}$ and $\widehat{\mathbf{K}}_{33}$, respectively.

The CMS_χ method described in Section 2 can be easily applied on this setting to obtain the reduced-order system matrices $\mathbf{M}_n$ and $\mathbf{K}_n$ defined in (22). This is done by letting $\mathbf{\Psi}_{13} = \mathbf{0}$ and $\mathbf{\Phi}_1 = \mathbf{I}$ in the transformation matrices $\mathbf{U}$ and $\mathbf{V}_n$ defined in (8) and (9), namely

$$\mathbf{U} = \begin{matrix} \\ N_1 \\ N_2 \\ N_3 \end{matrix} \begin{pmatrix} \overset{N_1}{\mathbf{I}} & \overset{N_2}{} & \overset{N_3}{\mathbf{0}} \\ & \mathbf{I} & \mathbf{\Psi}_{23} \\ & & \mathbf{I} \end{pmatrix}, \quad \mathbf{V}_n = \begin{matrix} \\ N_1 \\ N_2 \\ N_3 \end{matrix} \begin{pmatrix} \overset{n_1}{\mathbf{I}} & \overset{n_2}{} & \overset{N_3}{} \\ & \mathbf{\Phi}_2 & \\ & & \mathbf{I} \end{pmatrix}$$

Let us refer it as the $\mathrm{CMS}_\chi^{\mathrm{P}}$ method for this special case. Before we compare the $\mathrm{CMS}_\chi^{\mathrm{P}}$ method to the OMR method [14], we include a high-level description of the OMR algorithm for the sake of completeness.

Algorithm 3: OMR method [*14*]

1. Compute the eigenpairs $(\lambda_j, \mathbf{\phi}_j)$ of the subsystem $(\mathbf{K}_{22}, \mathbf{M}_{22})$.
2. Sort the eigenpairs $(\lambda_j, \mathbf{\phi}_j)$ according to the highest norm of the *coupling matrices* $\mathbf{S}_j^{\mathrm{O}}$ in descending order, i.e.

$$\|\mathbf{S}_1^{\mathrm{O}}\| \geqslant \|\mathbf{S}_2^{\mathrm{O}}\| \geqslant \cdots \geqslant \|\mathbf{S}_{N_2}^{\mathrm{O}}\|$$

3. Retain first n_2 eigenpairs $(\lambda_j, \mathbf{\phi}_j)$ to define $\mathbf{\Phi}_2$.
4. Calculate $\mathbf{M}_{22}^{(n)}, \mathbf{M}_{23}^{(n)}, \mathbf{K}_{22}^{(n)}$ and $\mathbf{K}_{23}^{(n)}$:

$$\mathbf{M}_{22}^{(n)} = \mathbf{I}, \quad \mathbf{M}_{23}^{(n)} = \mathbf{\Phi}_2^{\mathrm{T}}\mathbf{M}_{23}, \quad \mathbf{K}_{22}^{(n)} = \mathbf{\Lambda}^{(n)}, \quad \mathbf{K}_{23}^{(n)} = \mathbf{\Phi}_2^{\mathrm{T}}\mathbf{K}_{23}$$

5. Update the interface matrices $\mathbf{M}_{33}$ and $\mathbf{K}_{33}$:

$$\widehat{\mathbf{M}}_{33} = \mathbf{M}_{33} - \mathbf{M}_{23}^{\mathrm{T}}\mathbf{M}_{22}^{-1}\mathbf{M}_{23} + (\mathbf{M}_{23}^{(n)})^{\mathrm{T}}(\mathbf{M}_{22}^{(n)})^{-1}\mathbf{M}_{23}^{(n)}$$

$$\widehat{\mathbf{K}}_{33} = \mathbf{K}_{33} - \mathbf{K}_{23}^{\mathrm{T}}\mathbf{K}_{22}^{-1}\mathbf{K}_{23} + (\mathbf{K}_{23}^{(n)})^{\mathrm{T}}(\mathbf{K}_{22}^{(n)})^{-1}\mathbf{K}_{23}^{(n)}$$

6. Form reduced system matrices $\mathbf{M}_n$, $\mathbf{K}_n$ as defined in (22).

The main differences between $\mathrm{CMS}_\chi^{\mathrm{P}}$ and OMR methods are as follows. First, before solving generalized eigenvalue problem, $\mathrm{CMS}_\chi^{\mathrm{P}}$ transforms $(\mathbf{M}, \mathbf{K})$ to Craig–Bampton form, whereas OMR does not do any transformation. Second, after the modal projection, OMR updates the interface blocks $\mathbf{M}_{33}$ and $\mathbf{K}_{33}$, whereas $\mathrm{CMS}_\chi^{\mathrm{P}}$ does not modify interface blocks at this point. Finally, we note that $\mathrm{CMS}_\chi^{\mathrm{P}}$ is under the Galerkin reduction framework, whereas OMR is not due to the special modification of interface blocks $\mathbf{M}_{33}$ and $\mathbf{K}_{33}$. $\mathrm{CMS}_\chi^{\mathrm{P}}$ modifies the interface blocks implicitly when transforming $(\mathbf{M}, \mathbf{K})$ to the Craig–Bampton form (13).

We recall the *coupling matrices* $\mathbf{S}_j$ of $\mathrm{CMS}_\chi^{\mathrm{P}}$ defined in (16)

$$\mathbf{S}_j = \frac{1}{\lambda_j}\widehat{\mathbf{M}}_{23}^{\mathrm{T}}\boldsymbol{\phi}_j\boldsymbol{\phi}_j^{\mathrm{T}}\widehat{\mathbf{M}}_{23}$$

where $\widehat{\mathbf{M}}_{23} = (\mathbf{M}_{23} - \mathbf{M}_{22}\mathbf{K}_{22}^{-1}\mathbf{K}_{23})$. On the other hand, *coupling matrices* $\mathbf{S}_j^{\mathrm{O}}$ shown in the OMR [14] are defined as

$$\mathbf{S}_j^{\mathrm{O}} = \lambda_j\mathbf{M}_{23}^{\mathrm{T}}\boldsymbol{\phi}_j\boldsymbol{\phi}_j^{\mathrm{T}}\mathbf{M}_{23} - \mathbf{M}_{23}^{\mathrm{T}}\boldsymbol{\phi}_j\boldsymbol{\phi}_j^{\mathrm{T}}\mathbf{K}_{23} - \mathbf{K}_{23}^{\mathrm{T}}\boldsymbol{\phi}_j\boldsymbol{\phi}_j^{\mathrm{T}}\mathbf{M}_{23} + \frac{1}{\lambda_j}\mathbf{K}_{23}^{\mathrm{T}}\boldsymbol{\phi}_j\boldsymbol{\phi}_j^{\mathrm{T}}\mathbf{K}_{23} \qquad (23)$$

It can be verified that both coupling matrices are symmetric rank-one matrices, namely

$$\mathbf{S}_j = \mathbf{s}_j\mathbf{s}_j^{\mathrm{T}} \quad \text{and} \quad \mathbf{S}_j^{\mathrm{O}} = \mathbf{s}_j^{\mathrm{o}}(\mathbf{s}_j^{\mathrm{o}})^{\mathrm{T}}$$

where

$$\mathbf{s}_j = \frac{1}{\sqrt{\lambda_j}}\widehat{\mathbf{M}}_{23}^{\mathrm{T}}\boldsymbol{\phi}_j \quad \text{and} \quad \mathbf{s}_j^{\mathrm{o}} = \sqrt{\lambda_j}\mathbf{M}_{23}^{\mathrm{T}}\boldsymbol{\phi}_j - \frac{1}{\sqrt{\lambda_j}}\mathbf{K}_{23}^{\mathrm{T}}\boldsymbol{\phi}_j$$

A notable difference between the coupling matrices of $\mathrm{CMS}_\chi^{\mathrm{P}}$ and those of the OMR is how the eigenvalues affect the coupling $\widehat{\mathbf{M}}_{23}$. More precisely, these eigenvalues in coupling matrices of CMS_χ have a reciprocal relation to those of OMR[‡]:

$$\mathbf{S}_j = \frac{1}{\lambda_j^2}\mathbf{S}_j^{\mathrm{O}}$$

The eigenvalues λ_j play a role as a weight for coupling matrices. The major computational costs of the $\mathrm{CMS}_\chi^{\mathrm{P}}$ are transforming to the Craig–Bampton form and computing the norms of coupling

---

[‡]It is sufficient to show that $\mathbf{s}_j = (1/\lambda_j)\mathbf{s}_j^{\mathrm{o}}$. In fact, note that $\mathbf{K}_{22}^{-1}\mathbf{M}_{22}\phi_j = (1/\lambda_j)\phi_j$, we have $\mathbf{s}_j = \left(1/\sqrt{\lambda_j}\right)\widehat{\mathbf{M}}_{23}^{\mathrm{T}}\phi_j = \left(1/\sqrt{\lambda_j}\right)(\mathbf{M}_{23}^{\mathrm{T}} - \mathbf{K}_{23}^{\mathrm{T}}\mathbf{K}_{22}^{-1}\mathbf{M}_{22})\phi_j = (1/\lambda_j)\left(\sqrt{\lambda_j}\mathbf{M}_{23}^{\mathrm{T}} - \left(1/\sqrt{\lambda_j}\right)\mathbf{K}_{23}^{\mathrm{T}}\right)\phi_j = (1/\lambda_j)\mathbf{s}_j^{\mathrm{o}}$.

matrices $\mathbf{S}_j$. The costs of the OMR method are modifying the interface blocks and computing the norms of coupling matrices $\mathbf{S}_j^O$. Transforming to the Craig–Bampton form has essentially the same computational cost as modifying the interface blocks. In Section 5, numerical examples show that the CMS$_\chi$-mode selection lead to more accurate results.

5. NUMERICAL EXPERIMENTS

In this section, we present two numerical examples to compare the CMS, CMS$_\chi$ and OMR mode selection strategies discussed in this paper. All numerical experiments were run in MATLAB on a Pentium IV PC with 2.6GHz CPU and 1GB of core memory.

5.1. BCS structural dynamics

In this example, we compare the results of frequency response analysis by the CMS and CMS$_\chi$ methods. The mass matrix $\mathbf{M}$ and stiffness matrix $\mathbf{K}$ of the system of the form (1) are BCSSTM06 and BCSSTK06 from structure dynamics analysis in the Harwell–Boeing collection [18]. The dimensions of these matrices are $N = 420$. After a reordering by METIS [19], $\mathbf{M}$ and $\mathbf{K}$ are dissected into two substructures coupled by a small interface block ($N_3 = 36$). Two subsystems are of dimensions $N_1 = 190$ and $N_2 = 194$, respectively. We compute all eigenpairs of two substructures in order to select the desired modes in CMS$_\chi$.

The left of Figure 2 shows the magnitude (in log of base 10) of the transfer function $\mathbf{H}(\omega)$ of the system Σ_N with $\mathbf{B} = \mathbf{L} = [\,1\ 0\ \dots\ 0\,]^T$. The transfer functions $\mathbf{H}_n^{CMS}(\omega)$ and $\mathbf{H}_n^{CMS_\chi}(\omega)$ of the reduced systems Σ_n, computed by CMS and CMS$_\chi$, are shown in the same plot. The dimension of the reduced-order system Σ_n obtained by CMS or CMS$_\chi$ is $n = 153$. The dimensions of subsystems I and II are $n_1 = 52$ and $n_2 = 65$, respectively. The relative errors of the computed transfer functions shown in right of Figure 2 indicate that $\mathbf{H}_n^{CMS_\chi}(\omega)$ is a much accurate approximation of $\mathbf{H}(\omega)$ than $\mathbf{H}_n^{CMS}(\omega)$, where the the relative error of the CMS method is defined as $|\mathbf{H}(\omega) - \mathbf{H}_n^{CMS}(\omega)|/|\mathbf{H}(\omega)|$,

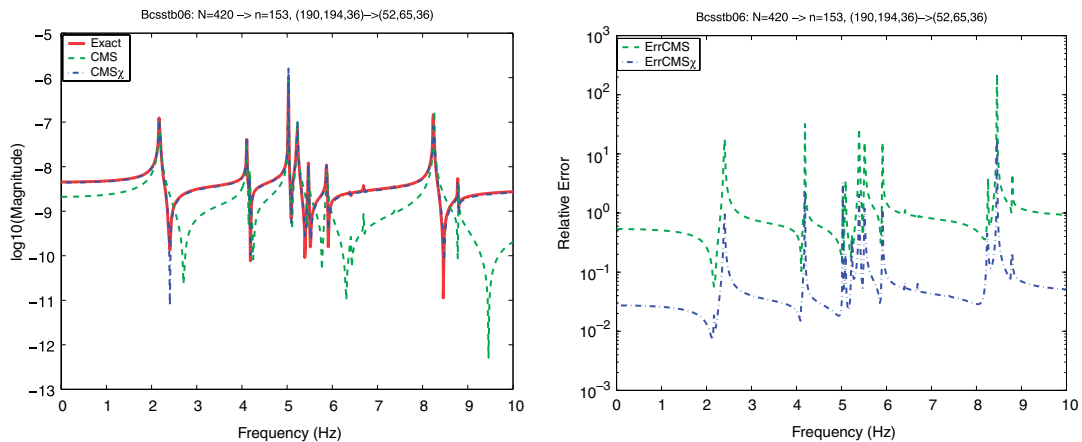Figure 2. Left: transfer functions. Right: relative errors.

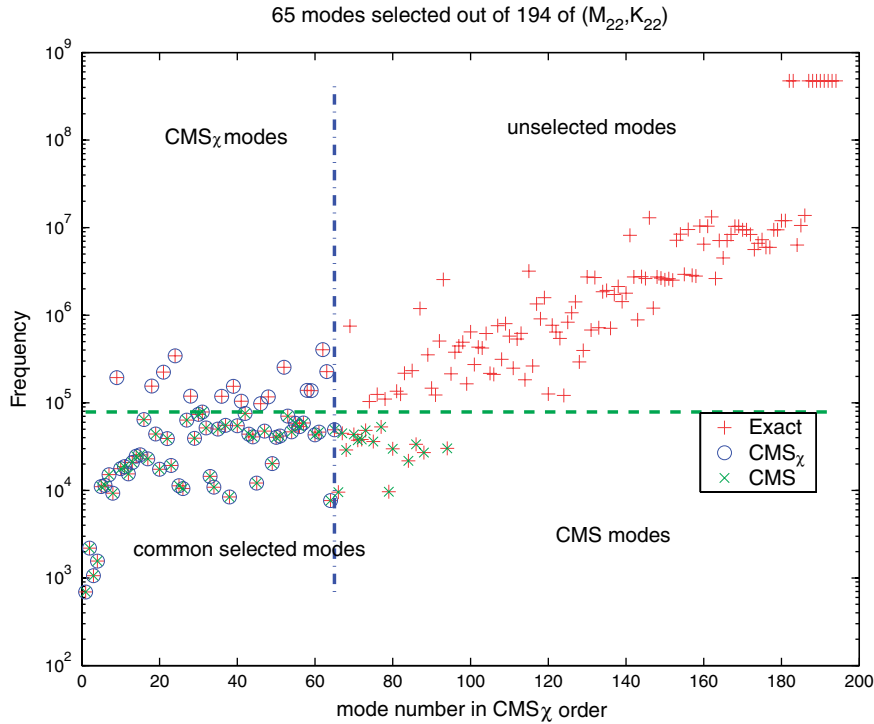Figure 3. Retained modes of system II by CMS and CMS$_\chi$.

and similarly the relative error of $\mathbf{H}_n^{\mathrm{CMS}_\chi}(\omega)$ is $|\mathbf{H}(\omega) - \mathbf{H}_n^{\mathrm{CMS}_\chi}(\omega)|/|\mathbf{H}(\omega)|$. By these two plots, it clearly shows that CMS$_\chi$ is more accurate than the CMS.

Figure 3 shows the eigenvalues of original subsystem II and the ones retained by CMS and CMS$_\chi$. Note that the numbers of eigenvalues of subsystems retained by the two methods are the same. CMS simply takes the lowest frequency eigenvalues in order. On the other hand, CMS$_\chi$ skips some of the low frequency eigenvalues, and selects a few higher frequency eigenvalues to take into the account of coupling effects between the subsystems and the interface.

5.2. The vibrating membrane problem

In this example, we compare the performance of CMS$_\chi$ and OMR methods for transient analysis of a simple lateral motion of a linear flat membrane. We use the same example as described in [13, 14]. The governed equation is the standard wave equation

$$\nabla^2 u = \ddot{u}$$

where u is the lateral displacement. The geometry of the membrane is shown in Figure 4. The substructure I is the left 3×3 square labelled as Ω_1, and the substructure II is the right hexagon labelled as Ω_2. The interface between them is the segment labelled as Γ. The sides with solid lines are fixed, whereas all the other sides (dash lines) are free. The initial velocity is zero everywhere. The initial displacement is a function changing linearly from $u = 0$ along the line
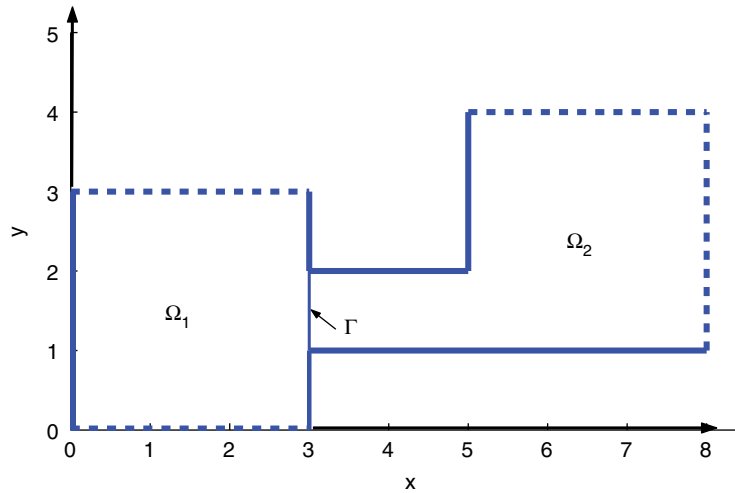
Figure 4. The geometry of the membrane problem.

$x = 0$ to $u = 1$ along the lines $x = 0.5$ to $u = 0$ again along the line $x = 1$. After the line $x = 1$, the initial displacement is zero everywhere.

After discretization by square bilinear finite elements of size 0.1×0.1, the degree of freedoms of the whole system Σ_N is $N = 1988$ and that of subsystems I, II and interface are $N_1 = 899$, $N_2 = 1080$ and $N_3 = 9$, respectively. We use a Newmark trapezoidal time-integration scheme [20] with the time-step $\Delta t = 0.01$ to solve both the original problem Σ_N and the reduced problems Σ_n with the given initial conditions. All eigenpairs of subsystem II are computed for the mode selection.

Figures 5(a)–(f) show the solutions u as a function of x for the fixed $y = 1.5$ for the full-order model, the reduced-order systems with $n_2 = 50$ using CMS$_\chi$ and OMR at time $t = 2, 4, 10, 12, 18$ and 25. The OMR results reported in [13] are essentially reproduced here. In these figures, the CMS$_\chi$ produces slightly more accurate solutions than the OMR method. However, the advantage of the CMS$_\chi$ is clearly shown for long time simulation, see Figures 6(a)–(d) at time $t = 35, 50, 75$ and 100.

6. CONCLUDING REMARKS

A coupling matrices-based mode selection criterion for the popular CMS method is presented in this paper. It is derived based on moment-matching principle. This work is motivated by the recent work of Givoli *et al.* [13, 14], in which the term 'coupling matrices' is coined. Our mode selection criterion is compatible to the one proposed by Givoli *et al.*, which uses Dirichlet-to-Neumann (DtN) map as an analysis tool. The performance improvement of the new mode selection criterion is demonstrated by numerical examples.

Although the numerical examples are convincing, it is still unclear at a theoretical level that how much information is lost by the frequency domain approximation and by matching only the first two moment vectors between the full and reduced models while minimizing the error in the
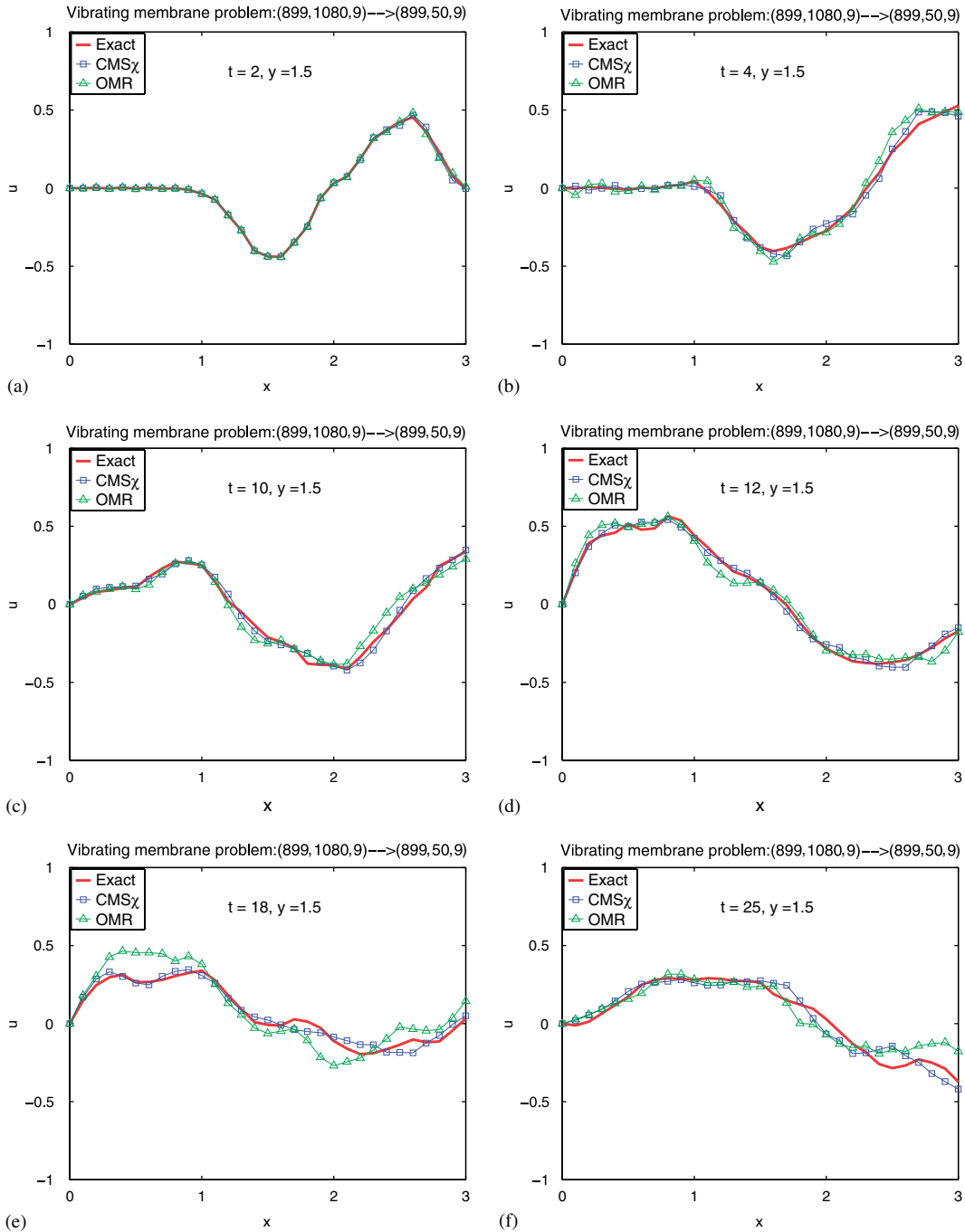
Figure 5. Solution u as a function of x with $y = 1.5$ for full model and reduced models obtained by CMS$_\chi$ and OMR at: (a) $t = 2$; (b) $t = 4$; (c) $t = 10$; (d) $t = 12$; (e) $t = 18$; and (f) $t = 25$.
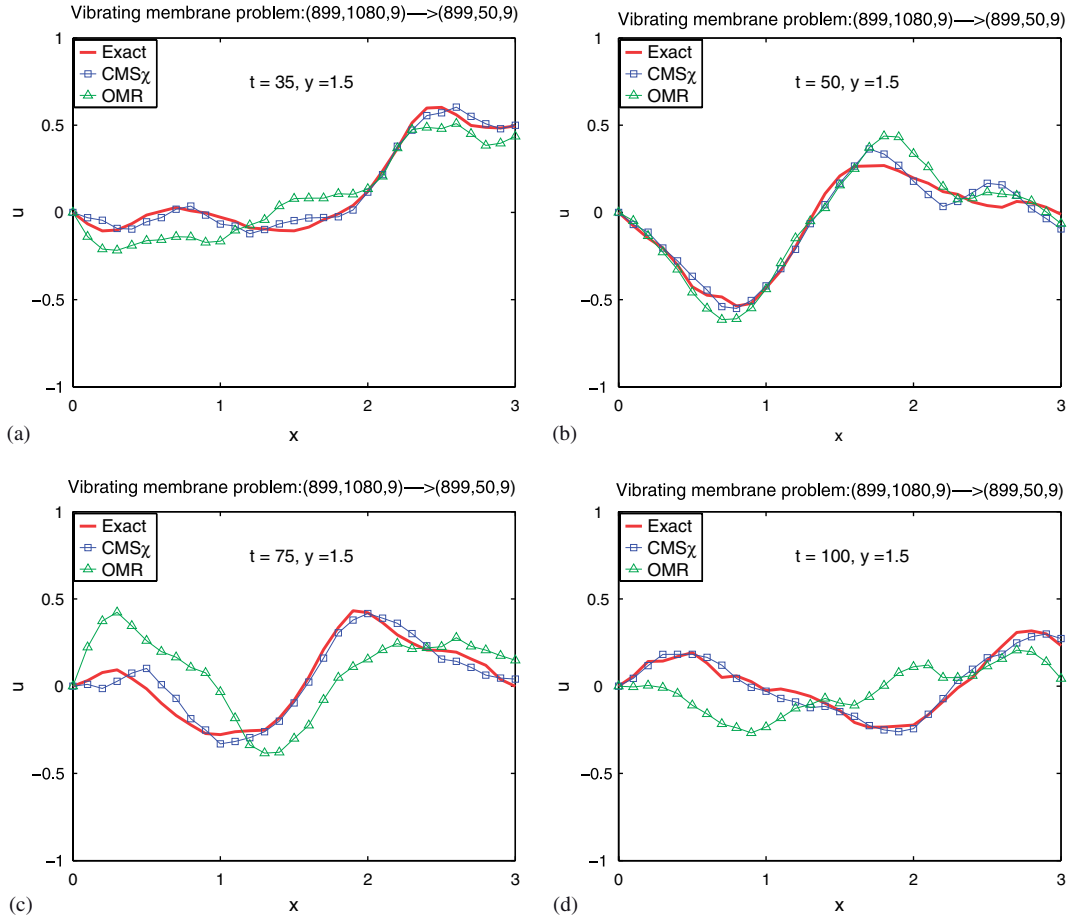
Figure 6. Solution u as a function of x for $y = 1.5$ for full model and reduced models obtained by CMS_χ and OMR at time: (a) $t = 35$; (b) $t = 50$; (c) $t = 75$; and (d) $t = 100$.

third moment vector. Furthermore, it is also unclear what is the implication of this approximation in time domain. A theoretical justification is a subject of further study.

We should note that the coupling matrices-based mode selection costs more than the standard one, since some extra eigenpairs of the subsystems are typically required. If the sizes of subsystems are moderate, the extra cost may not be significant measured by the CPU time. Multilevel substructuring with an optimal mode selection is a subject of future study. It is worth noting that modal reduction methods as discussed in this paper are generally less accurate and efficient than Krylov subspace-based reduction methods. A Krylov subspace-based substructuring method is in progress.

ACKNOWLEDGEMENTS

REFERENCES

1. Hurty WC. Dynamic analysis of structural systems using component modes. *AIAA Journal* 1965; **3**:678–685.
2. Craig Jr RR, Bampton MCC. Coupling of substructures for dynamic analysis. *AIAA Journal* 1968; **6**(7):1313–1319.
3. Hurty WC. Vibrations of structural systems by component-mode synthesis. *Journal of the Engineering Mechanics Division* (ASCE) 1960; **86**:59–69.
4. Craig Jr RR. Coupling of substructures for dynamic analysis—an overview. *AIAA-2000-1573*, 2000.
5. Bourquin F. Analysis and comparison of several component mode synthesis methods on one-dimensional domains. *Numerische Mathematik* 1990; **58**:11–34.
6. Bourquin F, d'Hennezel F. Intrinsic component mode synthesis and plate vibrations. *Computers and Structures* 1992; **44**:315–324.
7. Bourquin F, d'Hennezel F. Numerical study of an intrinsic component mode synthesis method. *Computer Methods in Applied Mechanics and Engineering* 1992; **97**:49–76.
8. Bennighof JK, Kim CK. An adaptive multi-level substructuring method for efficient modeling of complex structures. *Proceedings of the AIAA 33rd SDM Conference*, Dallas, Texas, 1992.
9. Bennighof JK. Adaptive multi-level substructuring method for acoustic radiation and scattering from complex structures. In *Computational Methods for Fluid/Structure Interaction*, Kalinowski AJ (ed.), vol. 178. AMSE: New York, 1993; 25–38.
10. Bennighof JK, Lehoucq RB. An automated multilevel substructuring method for eigenspace computation in linear elastodynamics. *SIAM Journal on Scientific Computing* 2004; **25**(6):2084–2106.
11. Kaplan MF. Implementation of automated multilevel substructuring for frequency response analysis of structures. *Ph.D. Thesis*, University of Texas at Austin, Austin, TX, December 2001.
12. Rugh WJ. *Linear System Theory* (2nd edn). Prentice-Hall: Englewood Cliffs, NJ, 1996.
13. Barbone PE, Givoli D. Optimal modal reduction of vibrating substructures. *International Journal for Numerical Methods in Engineering* 2003; **57**:341–369.
14. Givoli D, Barbone PE, Patlashenko I. Which are the important modes of a subsystem? *International Journal for Numerical Methods in Engineering* 2004; **59**:1657–1678.
15. Givoli D. *Numerical Methods for Problems in Infinite Domains*. Studies in Applied Mechanics, vol. 33. Elsevier: Amsterdam, 1992.
16. Keller JB, Givoli D. Exact non-reflecting boundary conditions. *Journal of Computational Physics* 1989; **82**: 172–192.
17. Bourquin F, Namar R. Decoupling and modal synthesis of vibrating continuous systems. In *Proceedings of the Ninth International Conference on Domain Decomposition Methods*, Bjørstad P, Espedal M, Keyes d (eds). Wiley: New York, 1996.
18. Duff IS, Grimes RG, Lewis JG. Users' guide for the Harwell–Boeing sparse matrix collection (release 1). *Technical Report RAL-92-086*, Rutherford Appleton Laboratory, December 1992. Available at the MatrixMarket: http://math.nist.gov/MatrixMarket
19. Karypis G, Kumar V. Metis—a software package for partitioning unstructured graphs, partitioning meshes, and computing fill-reducing orderings of sparse matrices—version 4.0. *Technical Report*, University of Minnesota, September 1998.
20. Hughes TJR. *The Finite Element Method*. Prentice-Hall: Englewood Cliffs, NJ, 1987.